International Journal of Naval Architecture and Ocean Engineering 14 (2022) 100473

Contents lists available at ScienceDirect

International Journal of Naval Architecture and Ocean Engineering

journal homepage: http://www.journals.elsevier.com/international-journal-of-naval-architecture-and-ocean-engineering/

Excessive acceleration simplified Operational Guidance

Ermina Begović, Guido Boccadamo, Barbara Rinauro, Gennaro Rosano*

Department of Industrial Engineering, University of Naples Federico II, Napoli, Italy

A R T I C L E I N F O

Article history:
Received 4 April 2022
Received in revised form
10 June 2022
Accepted 5 July 2022
Available online 10 July 2022

Keywords:
Excessive acceleration
Second generation intact stability criteria
Operational guidance
Effective wave slope coefficient
Froude-Krylov roll moment

A B S T R A C T

Excessive acceleration criterion, developed by the International Maritime Organization within the Second Generation Intact Stability Criteria, deals with lateral accelerations experienced by people onboard. Level 2 criterion considers the ship at zero speed in beam waves, neglects diffraction and gives the expressions for the Froude-Krylov roll moment. In this paper, the Level 2 procedure is generalized for any ship speed and heading by developing the expressions for the Froude-Krylov exciting roll moment as a function of the heading angle and introducing a variance preserving transformation from encounter to wave frequency. The proposed procedure can be easily implemented in a user's code to assess the simplified Operational Guidance without the use of commercial software. The proposed expression is validated comparing the Froude-Krylov roll moment with the one obtained by the 3-D potential code HydroStar®, referring to a barge and a bulk carrier. The bulk carrier is selected as test case to develop the simplified Operational Guidance according to the proposed procedure. A polar diagram representation is chosen to identify safe combinations of ship speeds and heading while a tabular representation is proposed for a given heading to identify the minimum ship speed to avoid large lateral accelerations, for the sea states reported in standard wave scatter table.

1. Introduction

The Second Generation Intact Stability Criteria (SGISC) were finalized in February 2020 by the International Maritime Organization (IMO) Sub-Committee on Ship Design and Construction (SDC), at its 7th session and Interim Guidelines were approved by the Maritime Safety Committee (MSC) at the end of the same year, (IMO MSC.1/Circ.1627 (2020)). This new set of regulations is intended to be included in Part A of the 2008 Intact Stability Code in following years, after an extensive testing phase.

The SGISC address five modes of intact stability failure in waves, divided in: restoring variation problems (parametric roll and pure loss of stability), manoeuvring related problems (surf-riding/broaching), stability under dead ship condition and excessive lateral accelerations.

The present paper focuses on the Excessive Acceleration (EA) criterion which deals with lateral accelerations experienced by people onboard, in considered locations along the ship. In some loading conditions, especially in ballast condition or ship partly loaded, which lead to low roll period, roll accelerations may magnify. The locations where crew or passengers may be present are of paramount importance since accelerations grow with the distance from the midship section and with the height above the roll axis.

The EA criterion was introduced in the SGISC framework later than the other four criteria, thanks to a proposal (IMO SLF 52/3/5, (2009)) of the German delegation, which highlighted that lateral accelerations due to synchronous rolling were not addressed by the SGISC. The proposal was submitted as a response to serious accidents associated to large roll angles and low roll periods on board of the containerships Chicago Express (2008), CCNI Guayas (2009) and Frisia Lissabon (2009), where people on board experienced transverse accelerations greater than the gravity acceleration g, and some crew members lost their life or suffered serious injuries.

Investigations (Federal Bureau of Marine Casualty Investigation, 2009 and 2011) showed that some parallelism exists between those three accidents, in terms of sailing conditions, loading conditions and hull geometry. Chicago Express was sailing partly loaded at the time of the accident while CCNI Guayas and Frisia Lissabon were in ballast condition. The loading conditions were characterized by large values of the metacentric height GM. Chicago Express was sailing in heavy weather with significant wave height around $7.5m$, with additional swell having a significant wave height of $3.0m$. The

* Corresponding author.
E-mail address: gennaro.rosano@unina.it (G. Rosano).
Peer review under responsibility of The Society of Naval Architects of Korea.

https://doi.org/10.1016/j.ijnaoe.2022.100473

wave heading was between 110° and 120°, while the vessel speed oscillated in the range from 3 to 5 *kn* at the time of the accident. Similar extreme weather conditions were experienced by CCNI Guayas and Frisia Lissabon, which were sailing at very low speed. In all accidents, low roll damping was one of the major reasons of the dramatic events, due to low ship speed. In addition, the vessels tended to adsorb high wave moments due to their large bow flare. Regarding this last point, numerical simulations (Federal Bureau of Marine Casualty Investigation, 2011) were performed on CCNI Guayas, whose length overall was around 208*m*, considering the ship in two different loading conditions characterized by nearly the same *GM*, but different draught and trim: the one at the time of the accident (ballast) and the other without ballast water. The first one had draughts at aft, midships and fore perpendicular equal to 7.45*m*, 5.70*m* and 3.95*m*, respectively, while the other had draughts equal to 7.35*m*, 3.86*m* and 0.37*m*, respectively. Simulations in waves, for a significant wave period $T_s = 9.5s$, showed that, despite the similar initial stability, the behaviour in waves was significantly different, with a substantial reduction of roll angles for the case without ballast water. Indeed, in that case the bow flare resulted out of the water and no excitation moment could be transmitted at bow.

The accidents' dynamics showed that the simultaneous combination of low roll damping, high initial stability and large bow flare trigger the inception of large lateral accelerations in beam or nearly beam seas. An increase in ship speed and a change in wave heading may prevent the ship against this phenomenon, which is mainly due to synchronous rolling, although a significative increase in ship speed could not be practicable due to severe sea state. In addition, the crew tends to avoid too high ship speeds to ensure the ship against slamming and water on deck or some combinations of speeds and headings to avoid other dangerous phenomena, as parametric rolling or loss of stability in waves. Therefore, a proper evaluation of the ship behaviour in waves should be made in the design phase, considering the various dynamic phenomena to which she could be prone to. If the ship is found vulnerable to one or more phenomena and changes in ship design are not feasible, the overall safety level of the vessel can be increased by means of Operational Measures (OM), (Bačkalov et al., 2016). IMO MSC.1/Circ.1228, (2008), represents a first attempt to implement OM in the intact stability rules currently in force. In the SGISC framework, OM are provided to the ship master as a support to decision-making on board and are divided in:

- Operational Limitations (OL) which limit ship operations to areas, routes and seasons or to maximum significant wave heights;
- Operational Guidance (OG) that define sailing conditions to be avoided in each considered sea state.

In recent years, many researchers explored the feasibility of their application. Rudaković and Bačkalov (2019) considered wind and wave measurements in Belgian coastal zone as alternative environmental conditions for OL development. They examined the behaviour of an inland container vessel sailing in North Sea coastal zone referring to Excessive acceleration and Dead ship condition criteria demonstrating that operational limitations of the vessel cannot be expanded by imposing a draught reduction to the selected sample ship when sailing in coastal zones. A significative improvement was obtained considering the effect on the metacentric height of unconventional vertical distributions of containers.

Applications of OG are reported in Belenky (2020), where a description of their derivation from Direct Stability Assessment or vulnerability criteria is given for all criteria, except for Dead ship condition to which OG do not apply. Polar plots representing OG are reported for the parametric roll failure mode.

Petacco and Gualeni (2020) applied OL to a Ro-Ro pax ferry operating in the Mediterranean Sea. The obtained results were represented in terms of minimum height of the centre of gravity to ensure the ship against lateral accelerations, for different draughts, showing that an increase in the design domain can be obtained introducing restrictions on the geographical area. Furthermore, Petacco et al. (2020) developed OG referring to lateral accelerations, for a megayacht according to IMO's procedure (IMO MSC.1/Circ.1627 (2020)).

Begović et al. (2021) developed OL related to maximum significant wave height and route for the bulk carrier considered in the present work. Different strategies were considered to define the scatter table to be used in the assessment when the route crosses several areas, each of which characterized by its own scatter table. It was shown that too conservative results may be returned taking into consideration only the most dangerous area in the route and, in some cases, results more severe than the ones obtained using the standard scatter table used in Level 2 assessment. A comparison between the assessment conducted weighting according to the route length or performing a simple arithmetic mean of the scatter tables associated to the crossed area along the route was performed, showing that the simple arithmetic mean could be a reasonable strategy only on short routes.

A first attempt toward the Direct Stability Assessment for the EA failure mode was made by Kuroda et al. (2019). The authors conducted experimental tests in irregular beam waves on a model of containership reproducing Chicago Express. Aim of the tests was to evaluate whether two numerical codes (one based on frequency domain calculations and the other one on time-domain simulations) were able to predict ship roll motion in short-crested irregular waves.

In the present paper, the EA Level 2 procedure, developed by the IMO for the ship at zero speed in beam waves, is generalized to account for all ship speeds and wave headings. An expression for the Froude-Krylov exciting roll moment calculation for any wave heading is proposed using a 2D approach, based on the standard methodology for the evaluation of the effective wave slope function implemented in Level 2, which associates to each ship transversal section an equivalent rectangular one through a transformation algorithm. The Froude-Krylov roll moment is obtained integrating the dynamic pressure of the incident wave over the calm water wetted surface of the equivalent rectangles. Aim of the paper is to provide a simple but accurate expression for the estimation of the exciting roll moment for any wave heading with the same level of complexity of Level 2 vulnerability criterion and minimum computational effort. This is in line with the philosophy of the regulations which should provide methods that can be applicable without the use of any commercial tool. The proposed methodology is validated comparing the amplitude of the Froude-Krylov roll moment with the one obtained by the 3-D potential code HydroStar®, referring to a barge and a bulk carrier, for different headings. A variance-preserving transformation is introduced to avoid discontinuities in the wave and response spectra in following and quartering waves. The OG are developed for the bulk carrier according to the proposed expression and polar diagrams are provided to identify safe combinations of ship speed and heading for relevant sea states. A tabular representation is proposed for a given heading to identify the minimum ship speed to avoid large lateral accelerations, for the sea states reported in standard wave scatter table. The results showed that, with the proposed method, the operability of the bulk carrier increases, and the operability domain is comparable to the one obtained by a commercial software.

2. SGISC Operational Measures

SGISC are structured with a multi-tiered approach with an increase in complexity from the lowest to highest level. The first two levels, Level 1 and 2, are named vulnerability criteria, while Level 3 is the so-called Direct Stability Assessment. The verification can start from any level and if the ship is found vulnerable, the next level, less conservative, can be applied, otherwise ship design must be changed or OM can be developed. OM are provided to the ship master as a support to decision-making on board and aim to reduce stability failures. As described in the flow chart in Fig. 1, OM are divided in OL which limit ship operations to areas, routes and seasons or to maximum significant wave heights, and in OG that define sailing conditions (combination of ship speed and heading) to be avoided in each considered sea state. OL are prepared following Level 1, Level 2, or the Direct Stability Assessment by replacing the North Atlantic wave scatter table by an another one related to an area, a route or a season, or by a limited wave scatter table obtained by cutting it up to a maximum significant wave height. OG can be provided following three different approaches: probabilistic, deterministic, and simplified. The probabilistic and deterministic approaches are based on the Direct Stability Assessment and require experimental tests or numerical simulations while the simplified OG are based on Level 2 vulnerability assessment, with appropriate changes depending on heading and speed variations.

OL related to maximum significant wave height and OG require weather forecast information for possible route changes to avoid dangerous situations. OM give an overview of the environmental conditions to be avoided for a considered loading condition, but if too many sea states are excluded the loading condition is considered not acceptable. IMO sets a limit equal to 20% as maximum value for the ratio between the sea states to be avoided and the total sea states taken into consideration.

For the EA criterion, the simplified OG requires the computation of the short-term failure indexes for all combinations of wave heading (from following to head seas) and ship speed (from zero to the service speed), in each sea state. Combinations for which the short-term index is higher than 10^{-6} should be avoided.

3. Excessive acceleration: Level 2 vulnerability criterion

EA criterion focuses on lateral accelerations generated by waves close to beam seas, which may excite the ship close to her natural roll frequency. This phenomenon is particularly felt in loading conditions characterized by a large transversal metacentric height (high initial stability), which leads to low roll period and, consequently, large roll accelerations. Lateral accelerations magnify with the distance from the roll axis, whose trace is indicated as R in Fig. 2, assumed to be located at the midpoint between the centre of gravity and the intersection point between the vertical line passing through the centre of gravity and the waterline (IMO MSC.1/Circ.1627, 2020).

Referring to Fig. 2, $\underline{a}$ is the acceleration in point P, located at a height equal to h above the roll axis. $\underline{a}$ is the results of various components: gravity acceleration, linear and centrifugal

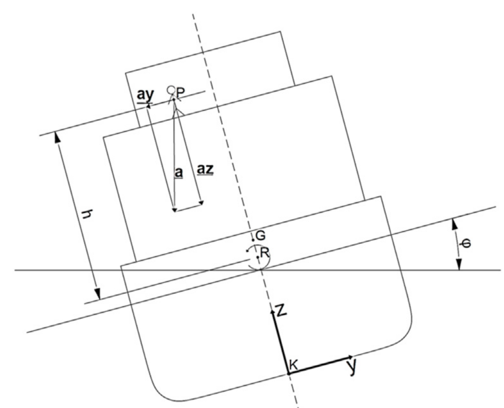

Fig. 2. Lateral acceleration.

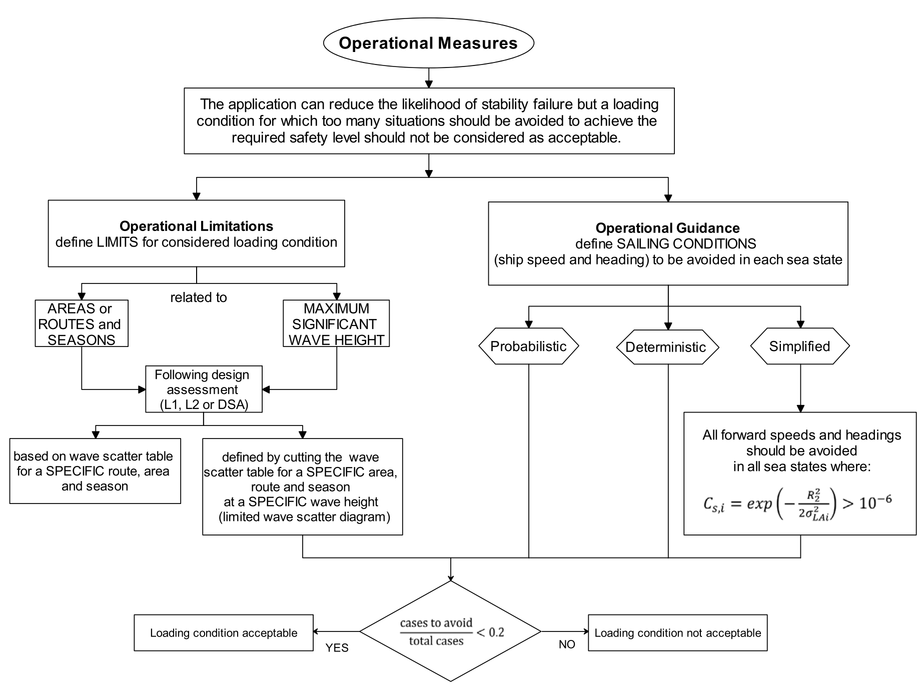

Fig. 1. OM procedures flowchart based on IMO Interim Guidelines (IMO MSC.1/Circ.1627, 2020).

accelerations caused by the roll motion itself, vertical and horizontal accelerations due to ship motions different from roll. These last ones are included in an approximate way in the 1-DOF model used in Level 2 procedure by means of a coupling factor k_L, which is a function of the longitudinal position of the calculation point of lateral acceleration (k_L is equal to 1 if the point is located between $0.2L$ and $0.65L$; it linearly increases outside this range, reaching its local maxima at fore and aft ends of the ship). The centrifugal acceleration is neglected. The projection of $\underline{a}$ on the y-axis, fixed to the ship, leads to the so-called lateral acceleration $\underline{a}_y$, whose amplitude is indicated as a_y.

In Level 2, the ship is assumed to be at zero speed in irregular beam waves and roll motion is modelled by means of a 1-DOF motion equation, which is non-linear in the damping term:

$$(I_{44}+A_{44})\ddot{\varphi}+M_D(\dot{\varphi})+C_{44}\varphi=F_{ex-4}(\omega t) \tag{1}$$

where: I_{44} is the mass moment of inertia; A_{44} is the added mass in roll; $M_D(\dot{\varphi})$ is the non-linear damping moment; $C_{44}=\Delta gGM$ is the restoring coefficient; Δ is the ship mass displacement; g is the gravity acceleration; GM is the transverse metacentric height; φ $\dot{\varphi}$, $\ddot{\varphi}$ are the roll angle, velocity and acceleration respectively; $F_{ex-4}(\omega t)$ is the exciting roll moment; ω is the wave frequency.

The exciting roll moment, $F_{ex-4}(\omega t)$, is described by the Froude-Krylov component, written in complex form as $\hat{F}_{FK-4}e^{i\omega t}=(a+ib)e^{i\omega t}$, being a and b the real and imaginary parts, expressed as follows (IMO SDC 8/5/Add.2, (2021)):

$$a=\rho g\zeta_a\iint_{S_{Body}} e^{kz}\cos(ky)n_4 dS \tag{2}$$

$$b=-\rho g\zeta_a\iint_{S_{Body}} e^{kz}\sin(ky)n_4 dS \tag{3}$$

where: ρ is the density of sea water; ζ_a is the wave amplitude; x, y and z are the coordinates of each point of the mean wetted hull surface of ship; S_{Body} is the mean wetted hull surface of ship; k is the wave number; $n_4=yn_3-zn_2$ is the normal vector of roll and n_2 and n_3 are the normal vectors in the $y-$ and $z-$ direction.

In Level 2 criterion, a simplified formulation is proposed for the calculation of a and b:

$$a=0 \tag{4}$$

$$b=\Delta gGMr(\omega)\frac{\omega^2}{g} \tag{5}$$

where $r(\omega)$ is the effective wave slope function, a linear function of the Froude-Krylov roll moment, F_{FK-4}, (IMO SDC 8/5/Add.2, (2021) and Rudaković et al. (2019)):

$$r(\omega)=\left|\frac{F_{FK-4}(\omega)}{\rho g\nabla GMk\zeta_a}\right| \tag{6}$$

being ∇ the volume of displacement. The computation of the effective wave slope function, Eq. (6), reduces to the evaluation of the Froude-Krylov roll moment amplitude F_{FK-4}. Different methods can be used to calculate it, based either on strip-theory or on 3D panel methods. In Level 2, a methodology based on strip theory, hereinafter “IMO's standard methodology”, for the evaluation of the effective wave slope function is proposed when more sophisticated tools are not available. This methodology associates an equivalent rectangle to each transversal section of the ship, through a transformation algorithm which keeps the underwater sectional area and the breadth at waterline.

The damping term in Eq. (1) is linearized introducing an equivalent linear roll damping factor B_e, such that $M_D(\dot{\varphi})=B_e\dot{\varphi}$. It can be evaluated either assuming its value at an angle of 15° or through a stochastic linearization, (IMO SDC 8/5/Add.2, 2021) which depends on the considered sea state. The stochastic linearization allows the computation of the equivalent linear roll damping coefficient, $\mu_e=\frac{B_e}{2(I_{44}+A_{44})}$, through an iterative procedure, once a set of extinction coefficients, linear μ, quadratic β, and cubic δ, is known. In particular, the equivalent linear roll damping coefficient is:

$$\mu_e=\mu+\sqrt{\frac{2}{\pi}}\beta\sigma_{\dot{\varphi}}(\mu_e)+\frac{3}{2}\delta(\sigma_{\dot{\varphi}}(\mu_e))^2 \tag{7}$$

where $\sigma_{\dot{\varphi}}$ is the standard deviation of roll rates.

Dividing both parts of Eq. (1) by (I_{44} +A_{44}) and introducing the damping factor, it becomes:

$$\ddot{\varphi}+2\mu_e\dot{\varphi}+\omega_\varphi^2\varphi=\frac{F_{FK-4}(\omega t)}{I_{44}+A_{44}}=\frac{(a+ib)}{I_{44}+A_{44}}e^{i\omega t} \tag{8}$$

where: $\frac{F_{FK-4}(\omega t)}{I_{44}+A_{44}}$ is the Froude-Krylov roll moment per unit mass moment of inertia; $\omega_\varphi=\sqrt{\frac{\Delta gGM}{I_{44}+A_{44}}}$ is the ship natural roll frequency.

The linearization of the roll motion equation allows its resolution in the frequency domain by means of spectral analysis. Therefore, the roll response, solution of Eq. (8), is harmonic and can be written as:

$$\varphi(t)=\widehat{\varphi}_a e^{i\omega t} \tag{9}$$

where: $\widehat{\varphi}_a$ is the complex roll amplitude, which contains both the magnitude and phase of the response. Therefore, the roll amplitude in complex form can be obtained:

$$\widehat{\varphi}_a=\frac{(a+ib)}{\left[-(I_{44}+A_{44})\omega^2+\Delta gGM\right]+i\omega B_e} \tag{10}$$

The real and imaginary parts of the roll amplitude are:

$$\varphi_r=\frac{a\left[\Delta gGM-(I_{44}+A_{44})\omega^2\right]+bB_e\omega}{\left[\Delta gGM-(I_{44}+A_{44})\omega^2\right]^2+(B_e\omega)^2} \tag{11}$$

and

$$\varphi_i=\frac{b\left[\Delta gGM-(I_{44}+A_{44})\omega^2\right]-aB_e\omega}{\left[\Delta gGM-(I_{44}+A_{44})\omega^2\right]^2+(B_e\omega)^2} \tag{12}$$

The transfer function of lateral acceleration may be derived from the roll response per unit wave amplitude, (Shigunov et al., 2011):

$$a_y\left(\omega\right)=k_L\left(g+h\omega^2\right)\varphi_a \tag{13}$$

where h is the height above the roll axis of the considered location, Fig. 2.

Therefore, the spectrum of lateral acceleration can be expressed as:

$$S_{a_y}(\omega)=\left(a_y(\omega)\right)^2 S_{zz}(\omega) \tag{14}$$

where $S_{zz}(\omega)$ is the wave energy spectrum. The environmental conditions are given by the standard wave scatter table (IACS Rec. No.34, 2001). To account for the wave directional spreading, a reduction factor, equal to 0.75, is introduced (IMO SDC 8/5/Add.1, 2021), giving finally the variance of lateral acceleration:

$$\sigma_{a_y}^2(\omega) = 0.75 \int_0^{+\infty} (a_y(\omega))^2 S_{zz}(\omega) d\omega \tag{15}$$

Assuming that lateral accelerations can be described by a Rayleigh distribution, a short-term excessive acceleration failure index $C_{s,i}$ is introduced:

$$C_{s,i} = exp\left(-\frac{R_2^2}{2\sigma_{a_y}^2}\right) \tag{16}$$

where $R_2 = 9.81\frac{m}{s^2}$. Such index is a measure of the probability of exceeding a lateral acceleration equal to the gravity acceleration, at the considered location on the ship, at least once in the considered sea state. The short-term failure index must be calculated for all combinations of significant wave height H_s and average zero-crossing period T_z reported in the scatter table and multiplied by the statistical frequency of occurrence of the corresponding sea state, W_i. The weighted sum of the short-term indexes allows the calculation of a long-term stability failure index C, which represent the vulnerability of the ship to experience excessive lateral accelerations at the considered location:

$$C = \sum_{i=1}^{N} W_i C_{s,i} \tag{17}$$

Level 2 vulnerability criterion is verified if the long-term stability failure index is lower than the limit value $R_{EA2} = 3.9 \cdot 10^{-4}$. This value was proposed by German delegation as the attained value of calculations performed on Chicago Express, considering her loading condition at the time of the accident (IMO SDC 4/5/13, 2016). Further information and comments on the EA criterion Level 1 and 2 limit values can be found in Boccadamo and Rosano (2019).

4. Excessive acceleration: simplified Operational Guidance

The simplified OG can be prepared based on the Level 2 vulnerability criterion, requiring the computation of the excessive acceleration short-term failure index $C_{s,i}$, defined by Eq. (16), for all ship speeds between zero and the service speed, and all wave directions, in the considered loading condition, for all sea states reported in the considered wave scatter table. For each sea state, combinations of ship speed and heading for which $C_{s,i} > 10^{-6}$ should be avoided. Therefore, Level 2, developed for the ship at zero speed in a beam seaway, has been modified to account for speed and wave heading. A summary of the modified Level 2 procedure is presented in the flowchart in Fig. 3, for a given sea state, where the output is the index $C_{s,i}$. Since OG are treated by means of spectral analysis, a variance preserving transformation is introduced to properly deal with quartering and following waves, Subsection 4.1, where all the frequency dependent terms are expressed in the wave frequency domain. In addition, the exciting Froude-Krylov roll moment, outlined in red in the flowchart, is described for any wave heading angle according to the formulation proposed in Subsection 4.2 and Appendix A.

4.1. Variance preserving transformation

In beam waves, the encounter frequency and the wave frequency are the same and the assessment is performed in the wave frequency range. If the ship advances with a constant speed V_s, different from zero, in long-crested waves with a constant direction of propagation μ, different from 90° or 270°, she will experience the motions with the encounter frequency, $\omega_e = \omega - \frac{\omega^2}{g}V_s cos\mu$, hence, spectral analysis has to be performed in the encounter frequency domain. In quartering or following waves the transformation from wave to encounter frequency is multi-valued and a variance-preserving transformation from the encounter to the wave frequency domain must be applied to calculate the spectral moments, Lewis (1989):

$$m_n = \int_0^{+\infty} \left|\omega - \frac{\omega^2}{g}V_s cos\mu\right|^n |\widehat{\varphi}_a(\omega)|^2 S_{zz}(\omega) d\omega \tag{18}$$

where m_n is the nth-order spectral moment of roll response and $\widehat{\varphi}_a$ is the transfer function of roll motion. The transformation may be used in two parts of the simplified OG development process: in the calculation of the variance of roll rates (stochastic linearization) and in the calculation of the variance of the spectrum of lateral acceleration. The variance of the spectrum of roll rates is:

$$\sigma_{\dot\varphi}{}^2 = \int_0^{+\infty} \left|\omega - \frac{\omega^2}{g}V_s \cos\mu\right|^2 |RAO_\varphi(\omega)|^2 S_{\alpha\alpha,e}(\omega) d\omega \tag{19}$$

where $S_{\alpha\alpha,e}(\omega)$ is the effective wave slope spectrum, calculated as $S_{\alpha\alpha,e}(\omega) = (r(\omega))^2 S_{\alpha\alpha}(\omega)$, being $r(\omega)$ the effective wave slope function, $S_{\alpha\alpha}(\omega)$ the wave slope spectrum; RAO_φ is the response amplitude operator of roll motion. The response amplitude operator of roll motion can be expressed in the wave frequency domain as follows, (St. Denis and Pierson (1951)):

$$RAO_\varphi(\omega, \mu_e) = \frac{\omega_\varphi^2}{\sqrt{\left[\omega_\varphi^2 - \left(\omega - \frac{\omega^2}{g}V_s cos\mu\right)^2\right]^2 + \left[2\mu_e\left(\omega - \frac{\omega^2}{g}V_s cos\mu\right)\right]^2}} \tag{20}$$

The variance of lateral acceleration spectrum can be expressed:

$$\sigma_{a_y}^2 = \int_0^{+\infty} (a_y(\omega))^2 S_{zz}(\omega) d\omega \tag{21}$$

where the transfer function is computed for the considered sailing condition and assuming the wave circular frequency as domain of integration.

4.2. Froude-Krylov exciting roll moment

The derivation of the expression for the Froude-Krylov roll moment calculation for any wave heading angle, to be used in the evaluation of the effective wave slope function according to Eq. (6), is described in detail in Appendix A. The procedure is 2D and it is based on the geometrical transformation of the IMO's standard methodology which transforms each transversal section of the ship into a rectangular one, (IMO SDC 8/5/Add.2, 2021). Therefore, the Froude-Krylov roll moment for any wave heading angle is obtained by means of formulas, which are exact for rectangles. The real and imaginary parts of the Froude-Krylov moment are also derived, to be used in the evaluation of the real and imaginary parts of the transfer function of roll motion.

The Froude-Krylov exciting roll moment is obtained via integration of the dynamic pressure of the incident wave over the calm

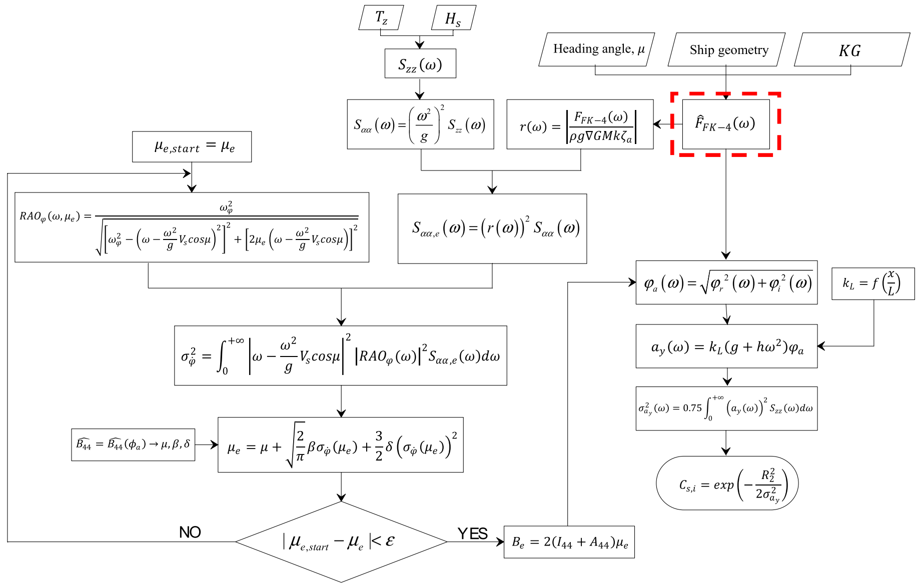

Fig. 3. Simplified OG development procedure.

water wetted surface of the body:

$$F_{FK-4}=\iint_{S_{Body}} p_I(yn_3-zn_2)dS \tag{22}$$

being p_I the dynamic pressure of the incident wave. Following strip theory assumptions and referring to the centre of gravity of the vessel, the integral can be rewritten as follows:

$$F_{FK-4}=\int_0^L\int_{C(x)} p_I[yn_3-(z-z_G)n_2]dCdx \tag{23}$$

where $z_G=OG=KG-d$ is the vertical distance between the centre of gravity and waterplane area; KG is the height of the centre of gravity above the keel line; $C(x)$ is the contour of the wetted surface at rest, at station x. According to the geometrical transformation, it reduces to the wetted contour of the equivalent rectangular section, having local draught $d(x)$ and breadth at waterline $B(x)$.

The Froude-Krylov exciting roll moment, eq. (23), can be expressed in complex form by means of eq. (A.2):

$$\widehat{F}_{FK-4}=\rho g\zeta_a e^{i\omega_e t}\int_0^L e^{-ikxcos\mu}\int_{C(x)} e^{kz}e^{-ikysin\mu}\times [yn_3-(z-z_G)n_2]dCdx \tag{24}$$

Eq. (24) can be rewritten as, see eq. (A.14):

$$\widehat{F}_{FK-4}=\rho g\zeta_a e^{i\omega_e t}\int_0^L e^{-ikxcos\mu}A(x)idx \tag{25}$$

where the quantity $A(x)$ is equal to:

$$A(x)=2\left[\left(\frac{d(x)}{k}+\frac{1}{k^2sin^2\mu}\right)e^{-kd(x)}-\left(\frac{1}{k^2}+\frac{z_G}{k}\right)\left(1-e^{-kd(x)}\right)\right] sin\left(k\frac{B(x)}{2}sin\mu\right)-\frac{B(x)}{ksin\mu}e^{-kd(x)}cos\left(k\frac{B(x)}{2}sin\mu\right) \tag{26}$$

Therefore, the Froude-Krylov roll moment amplitude can be expressed as:

$$F_{FK-4}=\rho g\zeta_a\sqrt{\left[\int_0^L \cos(kxcos\mu)A(x)dx\right]^2+\left[\int_0^L \sin(kxcos\mu)A(x)dx\right]^2} \tag{27}$$

Eq. (27) allows the computation of the effective wave slope function according to Eq. (6).

4.3. Froude-Krylov exciting roll moment validation

The validation of the formulas for calculation of the sectional and total Froude-Krylov roll moment, presented in the previous section and in Appendix A, is performed in three steps. First, the expression of the sectional Froude-Krylov roll moment is used to demonstrate that the formula reduces to the IMO's standard methodology if the beam seas case is considered, as shown in Appendix B. As second validation, the amplitude of the Froude-Krylov roll moment acting on a barge, for different headings, is compared against the results obtained by HydroStar® software, a 3D potential code developed by Bureau Veritas. Finally, the same comparison is performed considering the Froude-Krylov roll moment acting on a bulk carrier.

4.3.1. Barge

Eq. (A.12) represents the exact solution of the Froude-Krylov roll moment amplitude acting on a barge with zero trim. IMO's formulas and those proposed in the present work are exact for rectangular sections, therefore the results obtained with the present formulation and with more sophisticated methods should be nearly the same. A 20-m-long barge, whose principal dimension are given in Table 1, was considered to validate Eq. (A.12).

The Froude-Krylov roll moment was calculated both by the proposed formulation and by HydroStar® software. Four heading angles were considered to verify the formulation: 90°, 120°, 150°, 179°. The following convention was used for the wave heading angle: 0° and 180° correspond to following and head waves respectively. The curves show a good agreement between the two methodologies, Fig. 4.

4.3.2. Bulk carrier

A bulk carrier was considered as subject ship to check how much the Froude-Krylov exciting roll moment estimated with the modified procedure differs from the one calculated with a 3D potential flow method, which account for the actual ship geometry. The main dimensions and loading condition are reported in Table 2; the body plan is showed in Fig. 5, being 0 and 20 the stations located on the aft and forward perpendiculars respectively.

The comparison between the Froude-Krylov roll moment obtained by the modified IMO's formulation and HydroStar® is given in Fig. 6. A good agreement for frequencies up to 1.0 rad/s can be seen for all headings. For higher frequencies (i.e. for the waves with the period lower than 6 s) the difference tends to increase, since the wavelength and the ship breadth become comparable, see Fig. 7. The amplitudes match well at the ship natural roll frequency, represented by the dot-slash line in Fig. 6, around which the ship roll response tends to magnify.

5. Application of the proposed expression for Froude-Krylov roll moment evaluation

The bulk carrier introduced in Subsection 4.3.2 was considered as subject ship for the development of the simplified OG. The calculation point for the lateral acceleration was assumed at the wheelhouse, located at a distance x equal to 17.9m from aft perpendicular and at a height H equal to 19.47m above the keel line, Fig. 8. The ship was assumed with zero initial heel and trim. The ship service speed is 14.0 kn. The factor k_L, equal to 1.03, was calculated according to the formulation provided in IMO MSC.1/Circ.1627, (2020), and it was kept constant for all wave headings. According to regulations the EA assessment should be performed for a certain loading condition if the transverse metacentric height GM is higher than 8% of the ship breadth and the distance from the waterline of the highest location where crew or passengers may be located is higher than 70% of the ship breadth. Both conditions are verified for the subject ship which does not pass Level 1 and 2. OL related to route and maximum significant wave height were provided in a previous paper, (Begović et al., 2021), to permit ship operation under certain environmental conditions, without changes in ship design. The simplified OG have been developed in the present work to improve ship's operability performances.

The effect of ship speed on roll damping was considered introducing the lift damping component (assumed equal to zero in Level 2 assessment) in the calculation of damping coefficient by means of the Simplified Ikeda's Method, (Kawahara et al., 2009). Furthermore, due to the full hull form of the considered ship, the eddy damping component was calculated using the Simplified Ikeda's Method with the correction proposed by Rudaković and Bačkalov (2017). The effective wave slope function, whose knowledge is required to perform the stochastic linearization, was calculated according to Eq. (6), where the amplitude of the Froude-Krylov roll moment was calculated by Eq. (27). The variance-preserving transformation, according to the procedure reported in Subsection 4.1, was applied, for each sea state, to obtain the standard deviation of the spectrum of lateral acceleration, for the computation of the short-term stability failure index, Eq. (16). Calculations were performed in the wave frequency range $0.2 - 2.0\ rad/s$, i.e. for the wavelength from 15 to 1541 meters, respectively. The proposed procedure was implemented in Matlab® programming language.

Simplified OG were provided through a polar diagram representation where the headings 0° and 180° represent following and head seas respectively, while ship speeds from zero to the service speed are reported along the radius of the graphs. Safe combinations of ship speed and heading were identified for the sea states reported in the standard wave scatter table. In total 197 out of 272 combinations of significant wave height (H_s from 0.5m to 16.5m) and zero up-crossing period (T_z from 3.5s to 18.5s) have non-zero probability of occurrence.

Fig. 9 reports the results of OG application, for the sea states defined by four mean zero-crossing wave periods, 8.5, 9.5, 10.5, 11.5 s and three significant wave heights, 3.5, 5.5, 7.5 m. Each polar plot represents sea states having the same zero-crossing period and increasing significant wave heights. For each sea state, the contour defines the area inside which the ship is found vulnerable, therefore the sailing conditions outside the area identify the operability domain. Results show an expected reduction in the operational domain with the increase of the significant wave height.

The mean zero-crossing period has a significative influence on the ship response, for given significant wave height and heading. For the sea states showed in Fig. 9, the most severe results are for $T_z = 8.5s$. An increase of the mean zero-crossing period leads to a mitigation of the phenomenon, and the operability domain becomes wider. To examine more in depth the effect of the mean zero-crossing period, the transfer functions of lateral accelerations and the corresponding response spectra were obtained for the beam seas case, considering the significant wave height 5.5m and the periods 8.5, 9.5, 10.5, 11.5 s, Fig. 10. The Brethschneider wave energy spectrum was used to describe the environmental conditions. Wave spectra and transfer functions are drawn in the plot on the left. It can be noticed that the transfer functions show a peak in correspondence of the ship natural roll frequency, $\omega_r = 0.64\ rad/s$. The amplitude of the peak increases with the mean zero-crossing period. It is worth to underline that the transfer function of lateral acceleration depends on the sea state considered, because the equivalent

Table 1
Barge main dimensions.

MAIN DIMENSIONS			
Length	**L**	(m)	20.0
Breadth	**B**	(m)	10.0
Draught	**d**	(m)	5.0
Block coefficient	$\mathbf{C_B}$	-	1.0
Displacement	$\mathbf{\Delta}$	(t)	1025.0
Height of the centre of gravity	**KG**	(m)	2.5
Metacentric height	**GM**	(m)	1.67

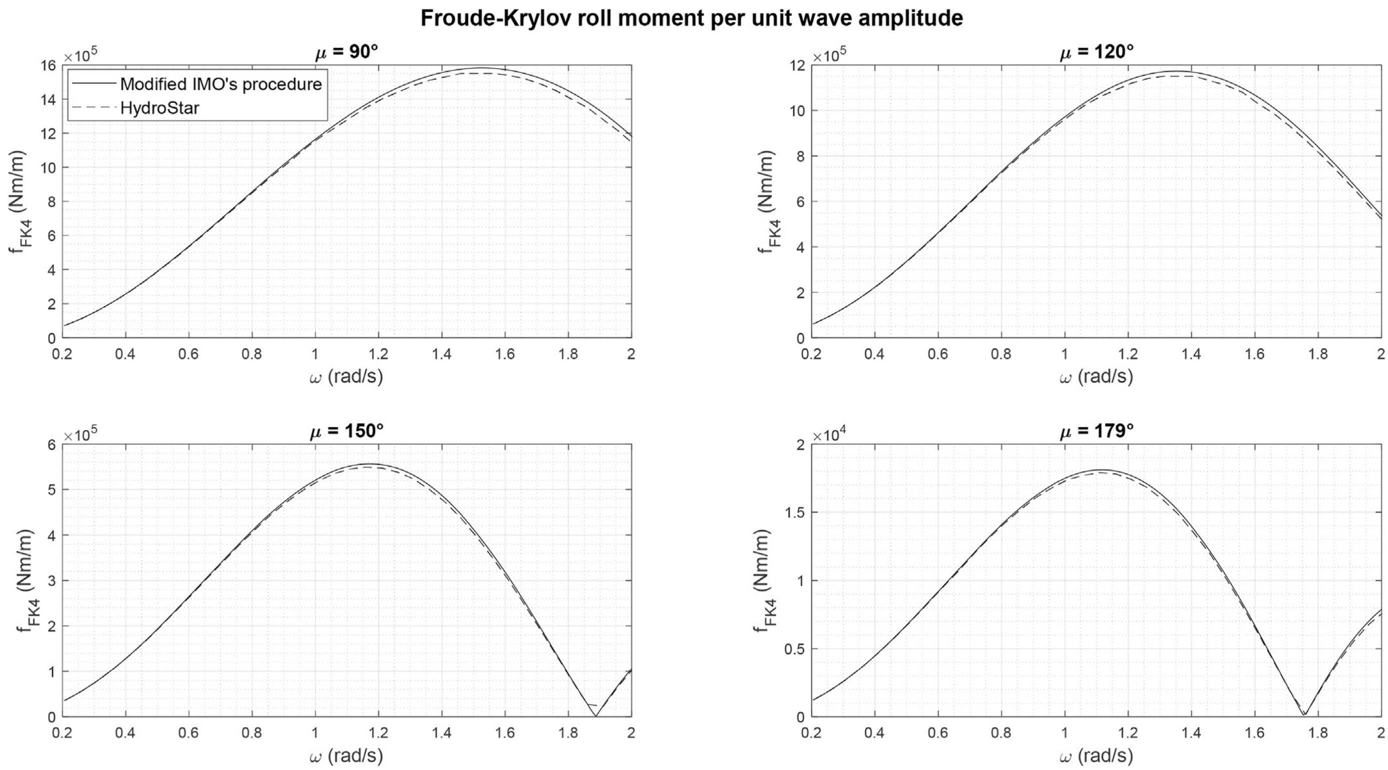

Fig. 4. Froude-Krylov roll moment acting on the barge for different wave headings.

Table 2
Bulk carrier main parameters.

MAIN DIMENSIONS			
Length	$\mathbf{L_{BP}}$	(m)	112.8
Breadth	**B**	(m)	16.8
Draught	**d**	(m)	6.7
Block coefficient	$\mathbf{C_B}$	-	0.81
Displacement	**Δ**	(t)	11622
Height of the centre of gravity	**KG**	(m)	5.38
Metacentric height	**GM**	(m)	1.71
Roll period	$\mathbf{T_r}$	(s)	9.83

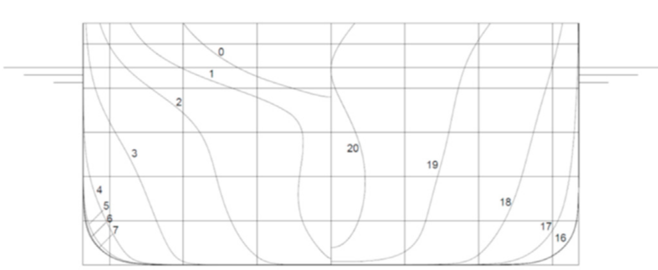

Fig. 5. Bulk carrier body plan.

damping factor is a function of the sea state.

Fig. 10 reports on the right side the response spectra of lateral acceleration, for the considered sea states, showing that, for the considered significant wave height, the sea state with the lowest zero-crossing period, i.e. 8.5s, is the one with the highest amount of energy around the peak of the transfer function, leading to the highest response in terms of lateral acceleration. The response spectra have the same shape, with a peak at the natural roll frequency.

Table 3 reports, for wave heading 120° and for each sea state, the ship speed, in knots, below which the short-term stability failure index $C_{S,i}$ is higher than the limit value 10^{-6}, identifying combinations of speed and heading that are not feasible. Cells coloured in red identify critical sea states, from the point of view of lateral acceleration, for any ship speeds. For these combinations of H_S and T_z different heading should be chosen. Cells coloured in green report zero forward speed identifying sea states for which ship will not suffer excessive lateral accelerations, for any ship speed. A comparison between the tabular forms of OG obtained with the modified IMO methodology and with HydroStar® has been reported, see Tables 3 and 4. The identified potentially dangerous sea states are the same. The tables show that the results provided by the modified procedure are more conservative compared with those obtained using the Froude-Krylov roll moment calculated by HydroStar software. Indeed, even though the modified methodology underestimates the roll moment at the higher frequencies, in the Excessive acceleration phenomenon most of the energy is concentrated around the natural roll frequency, where the roll moment is slightly overestimated by the modified procedure.

Similar tables could be derived for any heading angle,

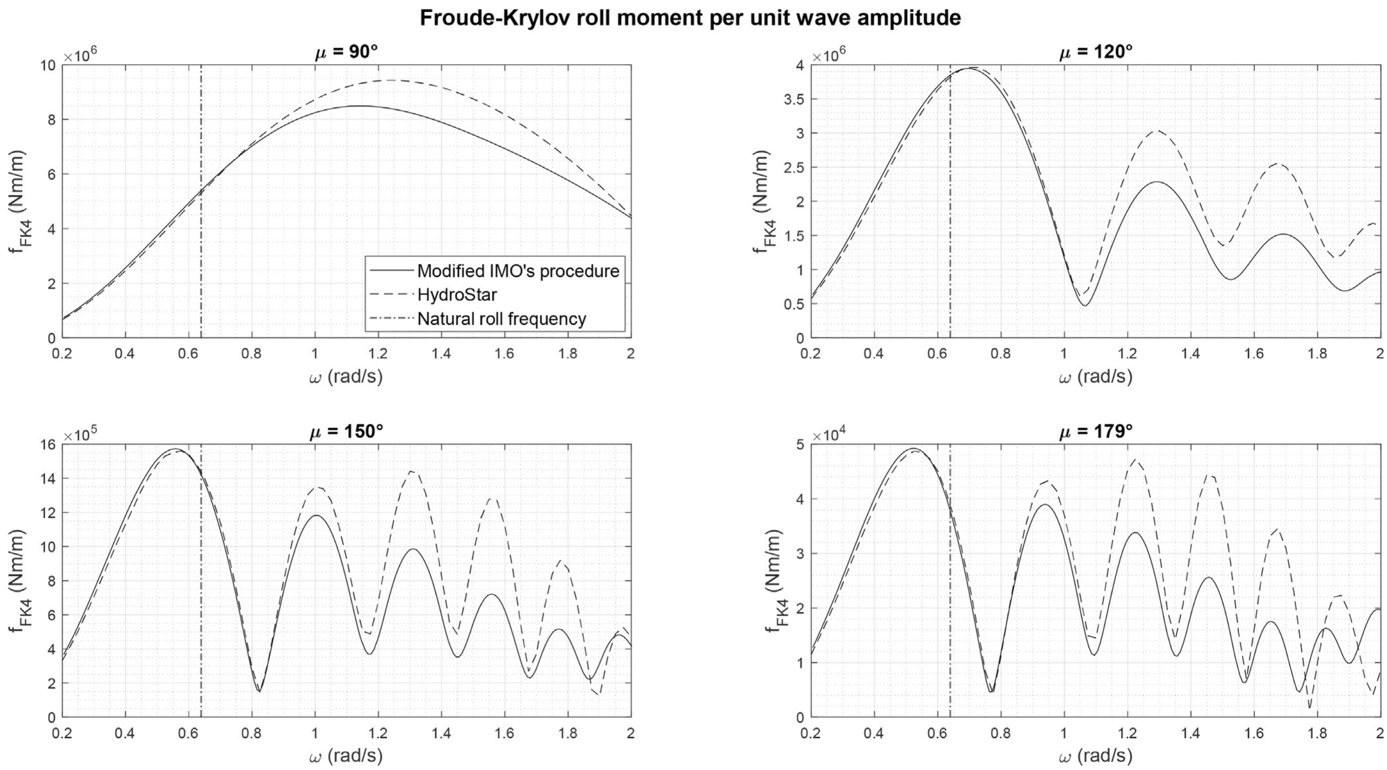

Fig. 6. Froude-Krylov roll moment acting on the bulk carrier for different wave headings as a function of the wave frequency.

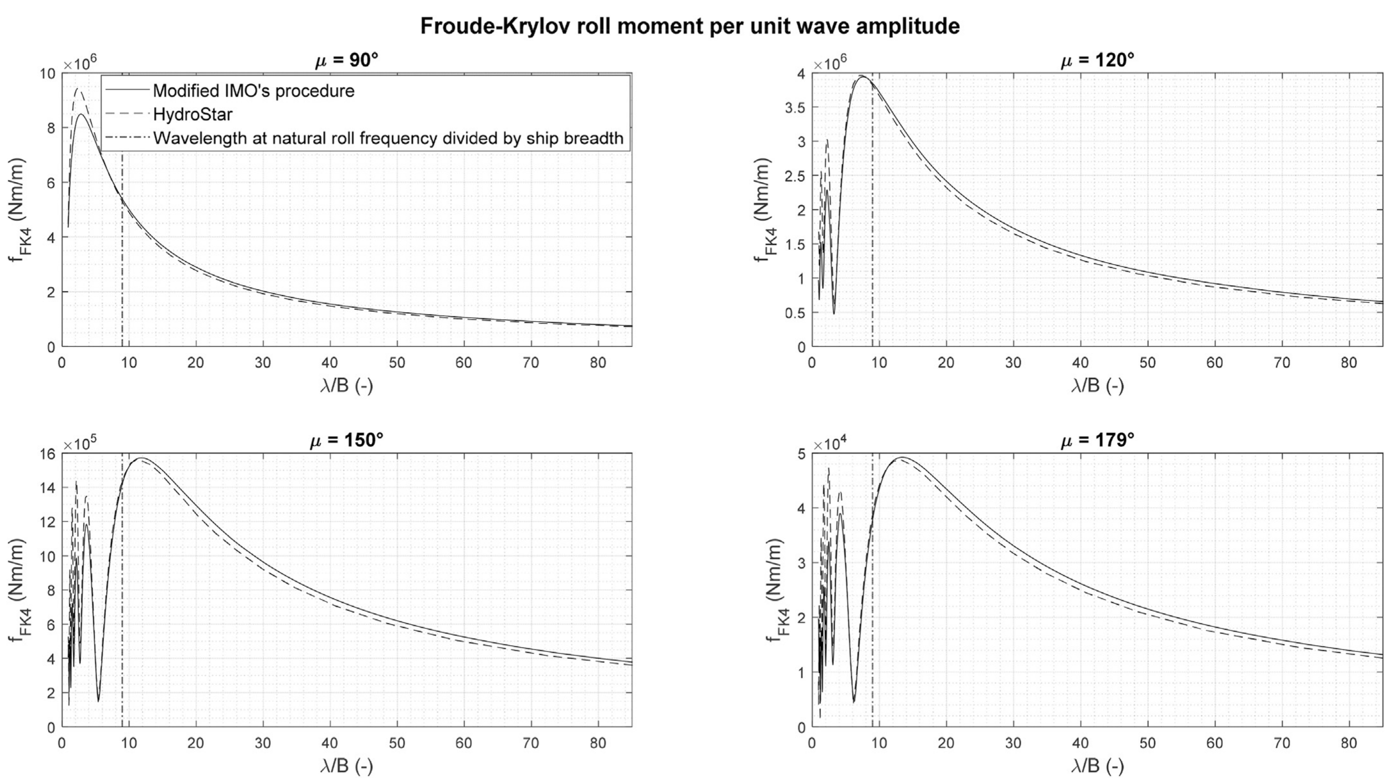

Fig. 7. Froude-Krylov roll moment acting on the bulk carrier for different wave headings as a function of the ratio λ/B.

identifying the corresponding speed limits, for each sea state.

As described in Section 2, a loading condition for which OG are provided is considered acceptable if the total duration of all situations which should be avoided to the total operational time is lower than 20%. The check was made by defining the sum of multiplications of the probability of encountering each sea state and a

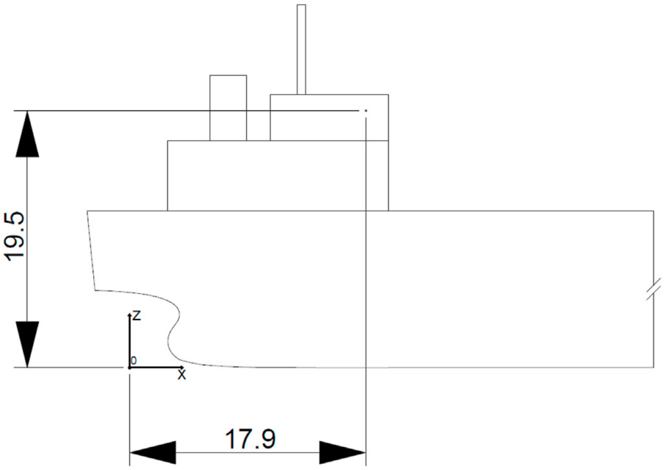

Fig. 8. Calculation point for lateral acceleration.

speed-heading factor which represents the ratio between the total cases of speed and heading combination to be avoided, and the total sailing cases. The North Atlantic wave scatter diagram was considered for the verification; the weighted sum, equal to 0.017, does not exceed 0.2 therefore, the loading condition is in compliance with the regulation and OG can be considered acceptable.

6. Conclusions

The present paper focuses on the Excessive acceleration criterion, one of the five stability failure modes within the SGISC. In Level 2 criterion, a methodology for the estimation of the so-called effective wave slope function, a linear function of the excitation moment, is introduced. The standard IMO's methodology consists of two parts: a geometrical transformation which associates an equivalent rectangular section to each ship transversal section, and a 2D strip-theory algorithm that uses formulas which are exact for rectangular sections and specific for the beam seas case. According

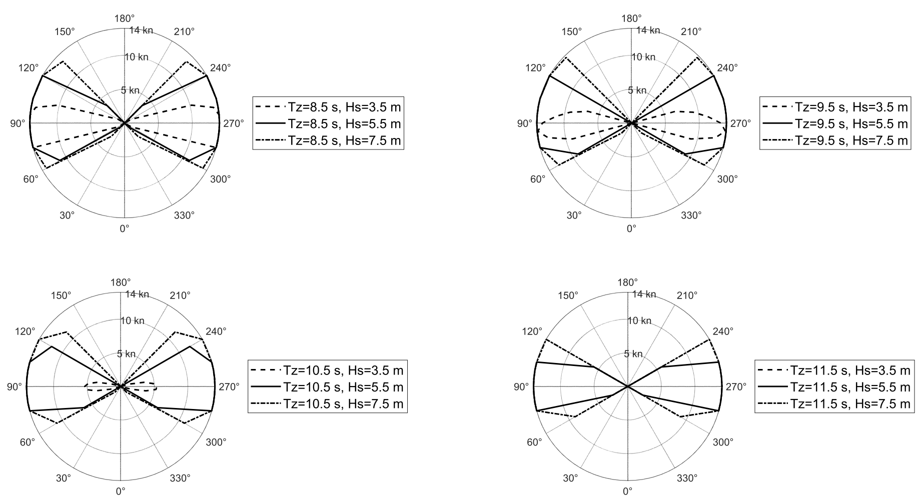

Fig. 9. Polar plot reporting the ship speeds to avoid the Excessive acceleration failure mode, for different sea states.

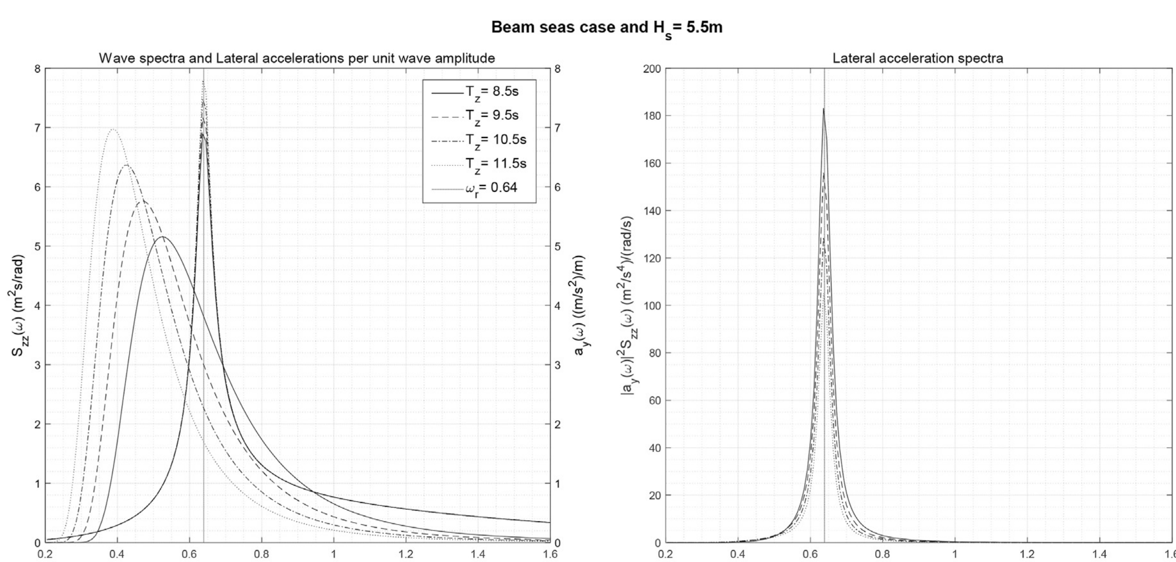

Fig. 10. Wave spectra, transfer functions of lateral acceleration and lateral acceleration spectra. Beam seas case and significant wave height 5.5 m.

Table 3
Minimum ship speed — Heading 120° - Modified IMO's procedure.

Excessive Acceleration Simplified Operational Guidance: Modified IMO's procedure (μ=120°)

Minimum speed		Tz (s)															
		3.5	4.5	5.5	6.5	7.5	8.5	9.5	10.5	11.5	12.5	13.5	14.5	15.5	16.5	17.5	18.5
	0.5	0.0	0.0	0.0	0.0	0.0	0.0	0.0	0.0	0.0	0.0	0.0	0.0	0.0	0.0	0.0	0.0
	1.5	0.0	0.0	0.0	0.0	0.0	0.0	0.0	0.0	0.0	0.0	0.0	0.0	0.0	0.0	0.0	0.0
	2.5	0.0	0.0	0.0	0.0	0.0	0.0	0.0	0.0	0.0	0.0	0.0	0.0	0.0	0.0	0.0	0.0
	3.5	0.0	0.0	0.0	0.2	2.4	1.1	0.0	0.0	0.0	0.0	0.0	0.0	0.0	0.0	0.0	0.0
	4.5	0.0	0.0	0.0	4.1	8.1	9.2	7.1	2.0	0.0	0.0	0.0	0.0	0.0	0.0	0.0	0.0
	5.5	0.0	0.0	0.7	7.1	12.4	14.0	14.0	11.9	5.8	0.0	0.0	0.0	0.0	0.0	0.0	0.0
	6.5	0.0	0.0	2.4	9.7	14.0	14.0	14.0	14.0	14.0	8.1	0.0	0.0	0.0	0.0	0.0	0.0
	7.5	0.0	0.0	3.7	12.0	14.0	14.0	14.0	14.0	14.0	14.0	9.5	0.0	0.0	0.0	0.0	0.0
Hs (m)	8.5	0.0	0.0	4.6	13.8	14.0	14.0	14.0	14.0	14.0	14.0	14.0	9.8	0.0	0.0	0.0	0.0
	9.5	0.0	0.0	5.6	14.0	14.0	14.0	14.0	14.0	14.0	14.0	14.0	14.0	9.3	0.0	0.0	0.0
	10.5	0.0	0.0	6.8	14.0	14.0	14.0	14.0	14.0	14.0	14.0	14.0	14.0	14.0	8.1	0.0	0.0
	11.5	0.0	0.0	7.7	14.0	14.0	14.0	14.0	14.0	14.0	14.0	14.0	14.0	14.0	14.0	6.7	0.0
	12.5	0.0	0.0	8.3	14.0	14.0	14.0	14.0	14.0	14.0	14.0	14.0	14.0	14.0	14.0	13.8	4.4
	13.5	0.0	0.0	9.4	14.0	14.0	14.0	14.0	14.0	14.0	14.0	14.0	14.0	14.0	14.0	14.0	11.3
	14.5	0.0	0.0	9.8	14.0	14.0	14.0	14.0	14.0	14.0	14.0	14.0	14.0	14.0	14.0	14.0	14.0
	15.5	0.0	0.0	10.8	14.0	14.0	14.0	14.0	14.0	14.0	14.0	14.0	14.0	14.0	14.0	14.0	14.0
	16.5	0.0	0.0	11.2	14.0	14.0	14.0	14.0	14.0	14.0	14.0	14.0	14.0	14.0	14.0	14.0	14.0

Table 4
Minimum ship speed — Heading 120° - F-K roll moment calculated by HydroStar.

Excessive Acceleration Simplified Operational Guidance: F-K roll moment calculated by HydroStar® software (μ=120°)

Minimum speed		Tz (s)															
		3.5	4.5	5.5	6.5	7.5	8.5	9.5	10.5	11.5	12.5	13.5	14.5	15.5	16.5	17.5	18.5
	0.5	0.0	0.0	0.0	0.0	0.0	0.0	0.0	0.0	0.0	0.0	0.0	0.0	0.0	0.0	0.0	0.0
	1.5	0.0	0.0	0.0	0.0	0.0	0.0	0.0	0.0	0.0	0.0	0.0	0.0	0.0	0.0	0.0	0.0
	2.5	0.0	0.0	0.0	0.0	0.0	0.0	0.0	0.0	0.0	0.0	0.0	0.0	0.0	0.0	0.0	0.0
	3.5	0.0	0.0	0.0	0.0	2.0	0.5	0.0	0.0	0.0	0.0	0.0	0.0	0.0	0.0	0.0	0.0
	4.5	0.0	0.0	0.0	4.0	7.5	8.2	6.2	0.8	0.0	0.0	0.0	0.0	0.0	0.0	0.0	0.0
	5.5	0.0	0.0	0.5	6.9	11.8	14.0	13.8	10.3	4.1	0.0	0.0	0.0	0.0	0.0	0.0	0.0
	6.5	0.0	0.0	2.3	9.5	14.0	14.0	14.0	14.0	13.2	6.4	0.0	0.0	0.0	0.0	0.0	0.0
	7.5	0.0	0.0	3.5	11.3	14.0	14.0	14.0	14.0	14.0	14.0	7.3	0.0	0.0	0.0	0.0	0.0
Hs (m)	8.5	0.0	0.0	4.2	13.4	14.0	14.0	14.0	14.0	14.0	14.0	14.0	7.5	0.0	0.0	0.0	0.0
	9.5	0.0	0.0	5.5	14.0	14.0	14.0	14.0	14.0	14.0	14.0	14.0	14.0	6.9	0.0	0.0	0.0
	10.5	0.0	0.0	6.7	14.0	14.0	14.0	14.0	14.0	14.0	14.0	14.0	14.0	14.0	6.0	0.0	0.0
	11.5	0.0	0.0	7.3	14.0	14.0	14.0	14.0	14.0	14.0	14.0	14.0	14.0	14.0	12.6	4.1	0.0
	12.5	0.0	0.0	8.3	14.0	14.0	14.0	14.0	14.0	14.0	14.0	14.0	14.0	14.0	14.0	10.7	3.0
	13.5	0.0	0.0	9.2	14.0	14.0	14.0	14.0	14.0	14.0	14.0	14.0	14.0	14.0	14.0	14.0	8.5
	14.5	0.0	0.0	9.7	14.0	14.0	14.0	14.0	14.0	14.0	14.0	14.0	14.0	14.0	14.0	14.0	14.0
	15.5	0.0	0.0	10.6	14.0	14.0	14.0	14.0	14.0	14.0	14.0	14.0	14.0	14.0	14.0	14.0	14.0
	16.5	0.0	0.0	11.1	14.0	14.0	14.0	14.0	14.0	14.0	14.0	14.0	14.0	14.0	14.0	14.0	14.0

to the Explanatory Notes of the SGISC, IMO SDC 8/5/Add.2, (2021), the standard methodology is recommended "since the vulnerability criteria is required to be applied with minimal computational efforts". In the present work, Level 2 criterion procedure was examined and extended to account for the effect of ship speed and wave heading. An expression for the Froude-Krylov roll moment was proposed to properly account for the wave exciting roll moment. The geometrical transformation was kept and the algorithm for the calculation of the effective wave slope function was updated to account for all wave headings. The Froude-Krylov roll moment in complex form was derived for the equivalent ship, whose transversal sections were substituted by rectangular ones.

The proposed formulation offers the following advantages: it can be easily implemented in a numerical code without requiring commercial software for its calculation; the methodology is coherent with the philosophy of the regulations which should provide simple but sufficiently accurate expressions to allow the calculations of the excitation moment without using any commercial tool, ensuring a sufficient level of safety; it is intended to be used in the development of the simplified Operational Guidance which should share the same methods and complexity of the Level 2 vulnerability criteria for the Excessive acceleration failure mode and the proposed version is an extension of a method already implemented in the rules with a quite limited increase in the computational effort.

The simplified OG were developed according to the proposed formulation, for each sea state reported in the standard wave scatter table, identifying safe combinations of ship speed and heading for which the short-term indexes were lower than the limit value 10^{-6}. Results were expressed as polar plots, identifying the minimum ship speed for any heading angle, below which the ship is found vulnerable. The effect of the significant wave height and zero-crossing wave period was investigated for relevant sea states. Additional results were reported for wave heading 120° in tabular form, defining the speed limits for each sea state. Similar tables could be obtained for different headings. It was verified that the total duration of all situations which should be avoided to the total operational time was lower than 20% to check if the OG were acceptable for considered loading condition.

The obtained results should be considered as a part of a comprehensive operability assessment which should consider all the phenomena to which the ship could be prone to. In addition, it should be verified that the allowable sailing conditions are feasible for the ship, since in heavy weather an increase in ship speed or a change in heading could be not practical due to speed loss in waves, reduced steering capabilities or occurrence of other dangerous phenomena.

Further improvement in ship operability could be obtained through the application of deterministic or probabilistic OG which account for at least four degrees of freedom of motion of the ships, relevant non-linearities and diffraction forces.

Declaration of competing interest

The authors declare that they have no known competing financial interests or personal relationships that could have appeared to influence the work reported in this paper.

Acknowledgments

The calculations by HydroStar® software have been possible thanks to the cooperation agreement between Bureau Veritas and the Department of Industrial Engineering of University of Naples Federico II.

Appendix A. Froude-Krylov exciting roll moment

A detailed derivation of Eqs. (25) and (27) is provided in this appendix.

A right-handed coordinate system $Oxyz$ moving with the forward speed of the ship V_s, assumed to be constant, is considered. The plane xy coincides with the mean water level, with x-axis pointing in the direction of ship's speed, and z-axis pointing upwards. At the instant $t=0$ the origin O is on the vertical through the centre of mass G. A regular wave propagates in the x' direction, inclined at an angle μ to the x-axis. The dynamic pressure of the incident wave, disregarding the non-linear term in Bernoulli's equation, can be expressed in the moving reference frame as, (Newman, 1977):

$$p_I = \rho g \zeta_a e^{kz} \sin(\omega_e t - kx\cos\mu - ky\sin\mu) \tag{A.1}$$

In complex form:

$$\widehat{p_I} = \rho g \zeta_a e^{kz} e^{i\omega_e t} e^{i(-kx\cos\mu - ky\sin\mu)} \tag{A.2}$$

The Froude-Krylov roll moment with respect to the centre of gravity, Eq. (23), is reported again in the following:

$$F_{FK-4} = \int_0^L \int_{C(x)} p_I [y n_3 - (z - z_G) n_2] dC dx \tag{A.3}$$

It can be expressed in complex form by means of Eq. (A.2):

$$\widehat{F}_{FK-4} = \rho g \zeta_a e^{i\omega_e t} \int_0^L e^{-ikx\cos\mu} \int_{C(x)} e^{kz} e^{-iky\sin\mu} [y n_3 - (z - z_G) n_2] dC dx \tag{A.4}$$

being $\widehat{F}_{FK-4}$ the complex form of the Froude-Krylov exciting roll moment. In beam seas, the real and imaginary parts reduce to (2) and (3), respectively. The complex form of the sectional Froude-Krylov roll moment per unit length is defined by the line integral over $C(x)$.

$$\widehat{f}_{FK-4} = \rho g \zeta_a \int_{C(x)} e^{kz} e^{-iky\sin\mu} [y n_3 - (z - z_G) n_2] dC \tag{A.5}$$

The line integral can be expressed, for a rectangular section having local draught d and breadth at waterline B, as a sum of three integrals:

$$\int_{C(x)} e^{kz} e^{-iky\sin\mu} [y n_3 - (z - z_G) n_2] dC = = -\int_{-d}^{0} e^{kz} e^{-ik\left(-\frac{B}{2}\right)\sin\mu} (z - z_G)(-1) dz + \int_{-\frac{B}{2}}^{\frac{B}{2}} e^{-kd} e^{-iky\sin\mu} y(-1) dy - \int_{-d}^{0} e^{kz} e^{-ik\frac{B}{2}\sin\mu} (z - z_G)(1) dz \tag{A.6}$$

Therefore:

$$\int_{C(x)} e^{kz} e^{-iky\sin\mu} [y n_3 - (z - z_G) n_2] dC = \left(e^{ik\frac{B}{2}\sin\mu} - e^{-ik\frac{B}{2}\sin\mu}\right) \int_{-d}^{0} e^{kz} (z - z_G) dz - e^{-kd} \int_{-\frac{B}{2}}^{\frac{B}{2}} e^{-iky\sin\mu} y dy \tag{A.7}$$

The sectional Froude-Krylov roll moment divided by $\rho g \zeta_a$ becomes:

$$\frac{\widehat{f}_{FK-4}}{\rho g\zeta_a}=\left(e^{ik\frac{B}{2}sin\mu}-e^{-ik\frac{B}{2}sin\mu}\right)\left[\left(\frac{d}{k}+\frac{1}{k^2sin^2\mu}\right)e^{-kd}-\left(\frac{1}{k^2}+\frac{z_G}{k}\right)\left(1-e^{-kd}\right)\right]-\frac{Bi}{2ksin\mu}e^{-kd}\left(e^{-ik\frac{B}{2}sin\mu}+e^{ik\frac{B}{2}sin\mu}\right) \tag{A.8}$$

Euler's formula, $e^{i\alpha}=cos\alpha+isin\alpha$, allows to rewrite Eq. (A.8) as follows:

$$\frac{\widehat{f}_{FK-4}}{\rho g\zeta_a}=\left\{2\left[\left(\frac{d}{k}+\frac{1}{k^2sin^2\mu}\right)e^{-kd}-\left(\frac{1}{k^2}+\frac{z_G}{k}\right)\left(1-e^{-kd}\right)\right]sin\left(k\frac{B}{2}sin\mu\right)-\frac{B}{ksin\mu}e^{-kd}cos\left(k\frac{B}{2}sin\mu\right)\right\}i \tag{A.9}$$

Eq. (A.9) is in complex form and its magnitude represents the sectional Froude-Krylov roll moment amplitude, divided by $\rho g\zeta_a$, for a generic heading angle μ:

$$\frac{f_{FK-4}}{\rho g\zeta_a}=2\left[\left(\frac{d}{k}+\frac{1}{k^2sin^2\mu}\right)e^{-kd}-\left(\frac{1}{k^2}+\frac{z_G}{k}\right)\left(1-e^{-kd}\right)\right]sin\left(k\frac{B}{2}sin\mu\right)-\frac{B}{ksin\mu}e^{-kd}cos\left(k\frac{B}{2}sin\mu\right) \tag{A.10}$$

Eq. (A.10) is not defined for heading angles equal to 0° or 180°. However, the sectional Froude-Krylov roll moment in following and head seas is equal to zero since Eq. (A.7) goes to zero.

The total Froude-Krylov roll moment can be obtained introducing the complex form of the sectional Froude-Krylov roll moment amplitude, Eq. (A.9), in Eq. (A.4). Then:

$$\widehat{F}_{FK-4}=\rho g\zeta_a e^{i\omega_e t}\int_0^L e^{-ikxcos\mu}\left\{2\left[\left(\frac{d}{k}+\frac{1}{k^2sin^2\mu}\right)e^{-kd}-\left(\frac{1}{k^2}+\frac{z_G}{k}\right)\left(1-e^{-kd}\right)\right]sin\left(k\frac{B}{2}sin\mu\right)-\frac{B}{ksin\mu}e^{-kd}cos\left(k\frac{B}{2}sin\mu\right)\right\}idx \tag{A.11}$$

An exact solution of Eq. (A.11) can be obtained if a barge with zero trim is considered. Indeed, terms in curly brackets are constant along x, and the Froude-Krylov roll moment amplitude can be written as:

$$F_{FK-4}=\rho g\zeta_a\left\{2\left[\left(\frac{d}{k}+\frac{1}{k^2sin^2\mu}\right)e^{-kd}-\left(\frac{1}{k^2}+\frac{z_G}{k}\right)\left(1-e^{-kd}\right)\right]sin\left(k\frac{B}{2}sin\mu\right)-\frac{B}{ksin\mu}e^{-kd}cos\left(k\frac{B}{2}sin\mu\right)\right\}\frac{1}{kcos\mu}\sqrt{\left[1-cos(kLcos\mu)\right]^2+\left[sin(kLcos\mu)\right]^2} \tag{A.12}$$

In the case of a ship, since breadth at waterline and local draught change along x, the terms in curly brackets in Eq. (A.11) are not constant. Therefore, the integral over the ship length must be discretized. The quantity $A(x)$ is introduced to emphasize the x-dependence of the terms in the brackets:

$$A(x)=2\left[\left(\frac{d(x)}{k}+\frac{1}{k^2sin^2\mu}\right)e^{-kd(x)}-\left(\frac{1}{k^2}+\frac{z_G}{k}\right)\left(1-e^{-kd(x)}\right)\right]sin\left(k\frac{B(x)}{2}sin\mu\right)-\frac{B(x)}{ksin\mu}e^{-kd(x)}cos\left(k\frac{B(x)}{2}sin\mu\right) \tag{A.13}$$

Then, Eq. (A.11) can be rewritten as:

$$\widehat{F}_{FK-4}=\rho g\zeta_a e^{i\omega_e t}\int_0^L e^{-ikxcos\mu}A(x)idx \tag{A.14}$$

The Froude-Krylov roll moment can be expressed as a sum of two integrals, separating the real and imaginary parts:

$$\widehat{F}_{FK-4}=\rho g\zeta_a e^{i\omega_e t}\left(i\int_0^L \cos(kxcos\mu)A(x)dx+\int_0^L \sin(kxcos\mu)A(x)dx\right) \tag{A.15}$$

Each integral can be calculated separately with a suitable integration method. Therefore, the Froude-Krylov roll moment amplitude can be expressed as:

$$F_{FK-4}=\rho g\zeta_a\sqrt{\left[\int_0^L \cos(kxcos\mu)A(x)dx\right]^2+\left[\int_0^L \sin(kxcos\mu)A(x)dx\right]^2} \tag{A.16}$$

Appendix B. IMO's standard methodology

In Level 2, the effective wave slope function is obtained by means of formulas, which are exact for rectangles. In the IMO's standard methodology, the effective wave slope function is defined as:

$$r(\omega)=\left|\frac{\int_L C(x)dx}{\nabla_{eq}\ GM}\right| \tag{B.1}$$

where:

$$C(x)=\begin{cases} 0\ if\ A_{eq}(x)=0\ and\ B_{eq}(x)=0 \\ A_{eq}(x)\left[K_1(x)+K_2(x)+F_1(x)OG_{eq}\right]\end{cases} \tag{B.2}$$

and:

$$K_1(x)=\frac{\sin\left(k\frac{B_{eq}(x)}{2}\right)}{\left(k\frac{B_{eq}(x)}{2}\right)}\frac{(1+kd_{eq}(x))e^{-kd_{eq}(x)}-1}{k^2\ d_{eq}(x)} \tag{B.3}$$

$$K_2(x)=-\frac{e^{-kd_{eq}(x)}}{k^2\ d_{eq}(x)}\left[\cos\left(k\frac{B_{eq}(x)}{2}\right)-\frac{\sin\left(k\frac{B_{eq}(x)}{2}\right)}{\left(k\frac{B_{eq}(x)}{2}\right)}\right] \tag{B.4}$$

$$F_1(x)=-\frac{1-e^{-kd_{eq}(x)}}{k\ d_{eq}(x)}\frac{\sin\left(k\frac{B_{eq}(x)}{2}\right)}{\left(k\frac{B_{eq}(x)}{2}\right)} \tag{B.5}$$

being $B_{eq}(x)$, $d_{eq}(x)$, $A_{eq}(x)$ the equivalent breadth at waterline, draught, and underwater area of each transversal sections, according to the transformation procedure, IMO SDC 8/5/Add.2, (2021). OG_{eq} is the height of the centre of gravity above the waterline.

IMO's formulas for the effective wave slope function may be obtained from the sectional Froude-Krylov roll moment amplitude, Eq. (A.10), considering the beam seas case, $\mu=90°$. It results:

$$\frac{f_{FK-4}}{\rho g\zeta_a}=2\left[\left(\frac{d}{k}+\frac{1}{k^2}\right)e^{-kd}-\left(\frac{1}{k^2}+\frac{z_G}{k}\right)\left(1-e^{-kd}\right)\right]sin\left(k\frac{B}{2}\right)-\frac{B}{k}e^{-kd}cos\left(k\frac{B}{2}\right) \tag{B.6}$$

Eq. (B.6) can be rearranged as follows:

$$\frac{f_{FK-4}}{\rho g\zeta_a}=Bd\left[\frac{2}{B}\frac{e^{-kd}}{k}sin\left(k\frac{B}{2}\right)+\frac{2}{Bd}\frac{e^{-kd}}{k^2}sin\left(k\frac{B}{2}\right)-\frac{2}{Bdk^2}sin\left(k\frac{B}{2}\right)+\frac{2}{Bd}\frac{e^{-kd}}{k^2}sin\left(k\frac{B}{2}\right)-\frac{2}{Bd}\frac{z_G}{k}sin\left(k\frac{B}{2}\right)+\frac{2}{Bd}\frac{z_G}{k}e^{-kd}sin\left(k\frac{B}{2}\right)-\frac{e^{-kd}}{kd}cos\left(k\frac{B}{2}\right)\right] \tag{B.7}$$

Dividing both parts of the equation for the wave number the following expression is obtained:

$$\begin{aligned}\frac{f_{FK-4}}{\rho gk\zeta_a}=Bd\Bigg[&\frac{2}{B}\frac{e^{-kd}}{k^2}sin\left(k\frac{B}{2}\right)+\frac{2}{Bd}\frac{e^{-kd}}{k^3}sin\left(k\frac{B}{2}\right)-\frac{2}{Bdk^3}sin\left(k\frac{B}{2}\right)+\frac{2}{Bd}\frac{e^{-kd}}{k^3}sin\left(k\frac{B}{2}\right)-\frac{2}{Bd}\frac{z_G}{k^2}sin\left(k\frac{B}{2}\right)\\ &+\frac{2}{Bd}\frac{z_G}{k^2}e^{-kd}sin\left(k\frac{B}{2}\right)-\frac{e^{-kd}}{k^2d}cos\left(k\frac{B}{2}\right)\Bigg]\end{aligned} \tag{B.8}$$

The sum of first, third and fourth elements in the square brackets returns the term $K_1(x)$ of the IMO' standard methodology, Eq. (B.3):

$$\frac{2}{B}\frac{e^{-kd}}{k^2}sin\left(k\frac{B}{2}\right)-\frac{2}{Bdk^3}sin\left(k\frac{B}{2}\right)+\frac{2}{Bd}\frac{e^{-kd}}{k^3}sin\left(k\frac{B}{2}\right)=\frac{sin\left(k\frac{B}{2}\right)}{k\frac{B}{2}}\left[\frac{(1+kd)e^{-kd}-1}{k^2d}\right]=K_1(x) \tag{B.9}$$

The sum of seventh and second elements returns the term $K_2(x)$, Eq. (B.4):

$$-\frac{e^{-kd}}{k^2 d}cos\left(k\frac{B}{2}\right)+\frac{2}{Bd}\frac{e^{-kd}}{k^3}sin\left(k\frac{B}{2}\right)=-\frac{e^{-kd}}{k^2 d}\left[cos\left(k\frac{B}{2}\right)-\frac{sin\left(k\frac{B}{2}\right)}{k\frac{B}{2}}\right]=K_2(x) \tag{B.10}$$

The sum of fifth and sixth elements returns the term which depends on the loading condition, i.e. the product between $F_1(x)$, Eq. (B.5), and OG, being $z_G = OG = KG - d$:

$$-\frac{2}{Bd}\frac{z_G}{k^2}sin\left(k\frac{B}{2}\right)+\frac{2}{Bd}\frac{z_G}{k^2}e^{-kd}sin\left(k\frac{B}{2}\right)=-\left[\left(\frac{1-e^{-kd}}{kd}\right)\right]\frac{sin\left(k\frac{B}{2}\right)}{k\frac{B}{2}}z_G=F_1(x)OG \tag{B.11}$$

Therefore, the sectional term $C(x)$, Eq. (B.2), is obtained:

$$\frac{f_{FK-4}}{\rho g k \zeta_a}=Bd[K_1(x)+K_2(x)+F_1(x)OG]=C(x) \tag{B.12}$$

Finally, the effective wave slope function according to IMO's standard methodology, is obtained:

$$r(\omega) = \left|\frac{F_{FK-4}(\omega)}{\rho g \nabla GM k \zeta_a}\right| = \left|\frac{\int_L f_{FK-4}(x)dx}{\rho g k \zeta_a \nabla\, GM}\right| = \left|\frac{\int_L C(x)dx}{\nabla\, GM}\right| \tag{B.13}$$

List of symbols

Greek symbols

β	Quadratic roll damping coefficient, *1/rad*
Δ	Ship mass displacement, *t*
δ	Cubic roll damping coefficient, *s/rad²*
ζ_a	Wave amplitude, *m*
λ	Wavelength, *m*
μ	Angle of heading, *rad*
μ	Linear roll damping coefficient, *1/s*
μ_e	Linear equivalent roll damping coefficient, *1/s*
$\widehat{\varphi}$	Complex roll amplitude, *rad*
φ	Roll angle, *rad*
$\dot{\varphi}$	Roll velocity, *rad/s*
$\ddot{\varphi}$	Roll acceleration, rad/s^2
φ_a	Roll amplitude in regular beam waves of unit amplitude at zero speed, *rad/m*
φ_i	Imaginary part of the roll amplitude in regular beam waves of unit amplitude at zero speed, *rad/m*
φ_r	Real part of the roll amplitude in regular beam waves of unit amplitude at zero speed, *rad/m*
ρ	Sea water mass density, t/m^3
σ_{a_y}	Standard deviation of lateral acceleration, m/s^2
σ_φ	Standard deviation of roll motion, rad^4/s^2
$\sigma_{\dot{\varphi}}$	Standard deviation of roll rates, rad^2/s
ω	Wave frequency, *rad/s*
ω_φ	Natural roll frequency, *rad/s*
ω_e	Encounter frequency, *rad/s*

Roman symbols

a	Real part of the Froude-Krylov roll moment, *Nm*
a_y	Lateral acceleration per unit wave amplitude, $(m/s^2)/m$
A_{44}	Added mass in roll, tm^2
b	Imaginary part of the Froude-Krylov roll moment, *Nm*

B	Breadth of the ship, *m*
B_e	Equivalent linear roll damping factor, *kNms*
C	Long-term excessive acceleration failure index
C_B	Block coefficient
$C_{s,i}$	Short-term excessive acceleration failure index
C_m	Midship section coefficient
C_{44}	Restoring coefficient, *Nm*
d	Mean draught, *m*
$\widehat{f}_{FK-4}$	Complex form of the sectional Froude-Krylov roll moment, *Nm/m*
F_{ex-4}	Magnitude of the exciting roll moment, *Nm*
F_{FK-4}	Magnitude of the Froude-Krylov roll moment, *Nm*
$\widehat{F}_{FK-4}$	Complex form of the Froude-Krylov roll moment, *Nm*
F_n	Froude number
g	Gravity acceleration, m/s^2
GM	Transverse metacentric height in calm water not corrected for free surface effect, *m*
h	Height above the roll axis of the calculation point of lateral acceleration, *m*
H	Height above the keel line of the calculation point of lateral acceleration, *m*
H_s	Significant wave height, *m*
I_{44}	Mass moment of inertia, tm^2
k	Wave number, *rad/m*
k_L	Factor taking into account simultaneous action of roll, yaw and pitch motions
KG	Height of the centre of gravity above the keel line, *m*
L	Length of the ship, *m*
$M_D(\dot{\varphi})$	Non-linear roll damping moment, *Nm*
n_2	Normal vector in the y-direction
n_3	Normal vector in the z-direction
n_4	Normal vector of roll
p_I	Dynamic pressure of the incident wave, N/m^2
$\widehat{p}_I$	Complex form of the dynamic pressure of the incident wave, N/m^2
r	Effective wave slope function
RAO_φ	Response Amplitude Operator
S_{a_y}	Spectrum of lateral acceleration, $(m^2/s^4)/rad/s$
$S_{\alpha\alpha}$	Spectrum of the wave slope, $rad^2/rad/s$
$S_{\alpha\alpha,e}$	Spectrum of the effective wave slope, $rad^2/rad/s$
S_φ	Spectrum of roll motion, $rad^2/rad/s$
S_{ZZ}	Wave frequency spectrum, m^2s/rad
T_r	Natural roll period of the ship, *s*
T_z	Mean zero up-crossing wave period, *s*
V_s	Ship speed, *m/s*
W_i	Weighting factor for the short-term environmental conditions
x	Longitudinal distance from aft perpendicular of the calculation point of lateral acceleration, *m*
z_G	Vertical distance between the centre of gravity and the waterplane area, *m*

Abbreviations

EA	Excessive acceleration
IMO	International Maritime Organization
OG	Operational Guidance
OL	Operational Limitations
OM	Operational Measures
SDC	Sub-committee on Ship Design and Construction
SGISC	Second Generation Intact Stability Criteria

References

Bačkalov, I., Bulian, G., Rosén, A., Shigunov, V., Themelis, N., 2016. Improvement of ship stability and safety in intact condition through operational measures: challenges and opportunities. Ocean Eng. 120, 353–361. https://doi.org/10.1016/j.oceaneng.2016.02.011.

Begović, E., Boccadamo, G., Rinauro, B., Rosano, G., June 2021. *Case Studies of SGISC Operational Limitations for Pure Loss of Stability and Excessive Acceleration*, 1st International Conference on the Stability and Safety of Ships and Ocean Vehicles, pp. 7–11. Glasgow, Scotland, UK.

Belenky, V., 2020. Continued development of second generation intact stability criteria. In: Naval Surface Warfare Center. Carderock Division. West Bethesda, MD, USA.

Boccadamo, G., Rosano, G., 2019. Excessive acceleration criterion: application to naval ships. J. Mar. Sci. Eng. 7, 431. https://doi.org/10.3390/jmse7120431.

Federal Bureau of Marine Casualty Investigation, November 2009. Investigtation Report 510/08. Fatal Accident on Board the CMV CHICAGO EXPRESS during Typhoon “HAGUPIT” on 24 September 2008 off the Coast of Hong Kong. Hamburg.

Federal Bureau of Marine Casualty Investigation, June 2011. Investigtation Report 391/09. Fatal Accident on Board the CMV CCNI GUAYAS during Typhoon “KOPPU” on 15 September 2009 in the Sea Area of Hong Kong (Including Analysis of Serious Marine Casualty 520/09 Pilot Injured on Board the CMV FRISIA LISSABON on 16 October 2009 West of Bokum on the Westerems). Hamburg.

IACS – Recommendation No. 34, 2001/Corr. 2001. *Standard Wave Data*, IACS Rec.

IMO MSC.1/Circ.1228, 2008. Revised Guidance to the master for avoiding dangerous situations in adverse weather and sea conditions. London.

IMO MSC.1/Circ.1627, 2020. Interim Guidelines on the Second Generation Intact. Stability Criteria, London.

IMO SDC 4/5/13, *Comments on Documents SDC 4/5/1 and SDC 4/INF.4*. *Submitted by Germany*, London, 22 December 2016.

IMO SDC 8/5/Add.1, 4 October 2021. Development of explanatory Notes to the Interim Guidelines on second generation intact stability criteria. In: Report of the Correspondence Group (Part 2). London.

IMO SDC 8/5/Add.2, 4 October 2021. Development of explanatory Notes to the Interim Guidelines on second generation intact stability criteria. In: Report of the Correspondence Group (Part 3). London.

IMO SLF 52/3/5, 18 November 2009. Development of New Generation Intact Stability Criteria. Proposal with Regard to the Scope of New Generation Criteria. Submitted by Germany. London.

Kawahara, Y., Maekawa, K., Ikeda, Y., 2009. A simple prediction formula of roll damping of conventional cargo ships on the basis of Ikeda's method and its limitation. In: Proceedings of the 10th International Conference on Stability of Ships and Ocean Vehicles. St. Petersburg.

Kuroda, T., Hara, S., Houtani, H., Ota, D., 2019. Direct Stability assessment for excessive acceleration failure mode and validation by model test. Ocean Eng. 187. https://doi.org/10.1016/j.oceaneng.2019.106137.

Lewis, E.L., 1989. Principle of Naval Architecture – Volume III. Society of Naval Architects and Marine Engineers, Jersey City, NJ United States.

Newman, J.N., 1977. Marine Hydrodynamics. The Massachusetts Institute of Technology.

Petacco, N., Gualeni, P., 2020. IMO second generation intact stability criteria: general overview and focus on operational measures. J. Mar. Sci. Eng. 8 (7), 494. https://doi.org/10.3390/jmse8070494, 2020.

Petacco, N., Gualeni, P., Stio, G., 2020. Second Generation Intact Stability Criteria: Application of Operational Limitations & Guidance to a Megayacht Unit. Proceeding of 5th International conference on Maritime Technology and Engineering, Lisbon, Portugal.

Rudaković, S., Bulian, G., Bačkalov, I., 2019. Effective wave slope coefficient of river-sea ships. Ocean Eng. 192, 106427. https://doi.org/10.1016/j.oceaneng.2019.106427.

Rudaković, S., Bačkalov, I., 2019. Operational limitations of a river-sea container vessel in the framework of the second generation intact stability criteria. Ocean Eng. 183. https://doi.org/10.1016/j.oceaneng.2019.05.013.

Rudaković, S., Bačkalov, I., 2017. *On Application of Standard Methods for Roll Damping Prediction to Inland Vessels*, 16th International Ship Stability Workshop. Belgrade, Serbia.

Shigunov, V., Rathje, H., El Moctar, O., Altmayer, B., 2011. On the consideration of lateral accelerations in ship design rules. In: Proceedings of the 12th International Ship Stability Workshop. Washington D.C., USA.

St Denis, M., Pierson, W.J., 1951. On the motions of ships in confused seas. SNAME Trans. 61.